Plume Characterisation of a Single Source Electrospray for Micro Electronic Cooling

M.J. Gibbons, A.J. Robinson

Department of Mechanical & Manufacturing Engineering, Trinity College Dublin, Ireland

Development and optimization of two phase electrospray cooling is an undeveloped topic, in part due to unavailable knowledge of how the various electrical, geometrical, thermal and hydraulic parameters influence both average and local heat transfer coefficients. Electrospray cooling (EC) enables two phase cooling by utilizing Coulomb forces for energy efficient fluid atomization while at the same time offering enhanced heat transfer using very small volumes of fluid. This research aims to characterize local heat transfer for different nozzle sizes (d), source to target separation heights (H), volumetric flow rates (Q), and target surface heat fluxes (q''). The results show that the peak heat transfer coefficient and the region of enhanced radial cooling are dependent on separation height and cooling fluid flow rate with minor dependency on nozzle size for certain cases. Importantly, the results show that very high peak heat transfer enhancement over natural convection can be achieved with electrosprays with exceptionally low flow rates.

Keywords—Electrospray cooling, Thermal management, Electronic cooling

1 INTRODUCTION

Traditional fan-based and natural convection cooling has long been applied as the standard for thermal management in industrial and consumer electronics given their simplicity and robustness. The increasing expectations on small form factor electronics to be more compact while increasing performance has driven conventional natural convection and fan-based cooling technologies to a thermal management bottleneck. Effective thermal energy dissipation is crucial in maintaining a product's performance and long term reliability.

An emerging solution to this thermal management problem is electrospray cooling (EC). EC utilizes Coulomb forces for energy efficient fluid atomization. The generated droplets enable phase change cooling for the dissipation of the imposed heat fluxes. Charged liquid droplets are propelled from the nozzle to the target by a potential difference that exists between the source and target. The voltage potential required to induce EC is dependent on the cooling fluid properties and the spraying regime being implemented with very low additional energy requirements [1, 2]. By modifying certain parameters one can precisely control droplet size, distribution and associated heat transfer.

Electrospraying is an attractive proposition for cooling applications because it offers low profile liquid cooling performance for extremely low liquid flow rates, they do not require compressed air to generate the atomized spray and do not entail any significant additional electrical power to operate. This would make EC technology particularly attractive for space application, where size and weight restrictions are vital and there are no buoyancy forces for natural convection. Unlike conventional sprays, EC also enables almost complete avoidance of rebound losses, which reduces conventional spray efficiency, as a result of the Columbic attraction that exists between the charged coolant and the target [3, 4].

Corresponding author: Michael Gibbons
E-mail address: migibbon@tcd.ie

1.1 Research objectives

Although very sparse, there is prior research [5-8] that has shown that EC technology is a viable option as a thermal management solution for small form factor electronics. Feng and Bryan [5] were possibly the first to investigate two phase electrospray cooling. During their research they studied the heat transfer characteristics of two-phase impinging liquid cooling for different capillary tube arrays in an enclosed chamber. Their work showed that optimum heat transfer enhancement existed at lower heat fluxes (less than 30 W/cm^2). This condition corresponded to the ramified jet regime of spraying and resulted with an enhancement of 1.7 times over natural convection alone.

Wang and Mamishev [7, 8] further developed the field by exploring the interaction of nozzle spacing and the subsequent effect on the averaged heat transfer coefficient. A peak enhancement ratio of 1.87 was achieved for an 8 nozzle, 5mm spacing array at the

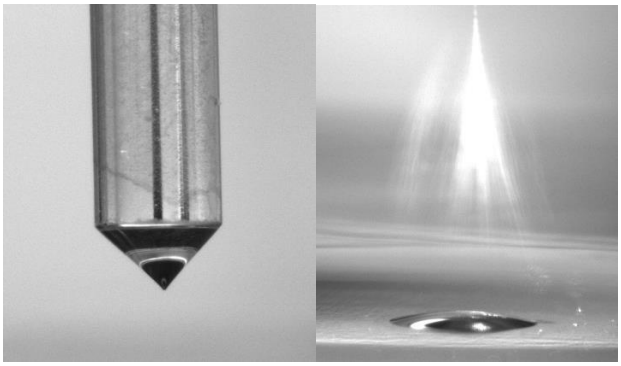

Fig 1 Electrospray cooling cone-jet mode, (left) Taylor cone, (right) spray plume

lowest heat flux. In their later research they developed multiple Nusselt number correlations for different geometric nozzle spacing and arrangements.

Deng and Gomez [6] demonstrated microfabricated multiple source arrays. An optimal average heat flux removal of 96 W/cm^2 with a cooling efficiency of 97% was achieved for the specified system.

Unlike past research highlighted above, all of which focused on surface averaged heat transfer coefficients for electrospray cooling, this research endeavors to be the first to investigate the heat transfer coefficient distributions resulting from single nozzle electrosprays in the cone-jet mode regime under evaporative cooling conditions. Specifically, ultra-low flow rates are studied. This was achieved using an ohmically heated thin foil and thermal imaging system in order to fully investigate and characterise the local cooling features of the electrospray under varied operating parameters.

2 BACKGROUND

In 1917 John Zeleny [1] first observed that the nature of liquid dipping and spraying changed under application of an electric field. It was not until 1964 that Geoffrey Taylor [9] provided a theoretical explanation for the "Taylor" cone-jet mode that Zeleny observed (Fig 1) [2, 7].

When a voltage is applied to a nozzle an electric field is established between the source and the target surface. This applied voltage induces charges within the working fluid. As the voltage is increased the electric field and the charge density also increases. At a critical voltage the induced Coulomb forces act on the charges in the working fluid resulting in the meniscus deforming into the shape of a cone (Fig 1). This cone is extended at its apex by a permanent jet which breaks into a stream of charged droplets to form a spray. These charged droplets repel each other causing drop dispersion i.e. spreading of the jet spray, and are then accelerated towards the target surface due to electrostatic forces [2]. If the applied voltage continues to increase a multi-jet mode of spraying will be induced [2, 10].

While the multi-jet mode enables greater surface area coverage, the droplets generated are of a poor consistency [8] and the cone creation and position on the nozzle are unpredictable. The cone jet mode in contrast is particularly appealing due to its stability, predictability and fine droplet creation [2].

3 EXPERIMENTAL SETUP

The experimental apparatus is shown in Fig 2 and a schematic of the rig design can be seen in Fig 3 for further clarification.

3.1 Electrospray System

Both the applied nozzle voltage and flow rate were supplied by a Profector Life Sciences Electrospray Controller (Fig 2). The voltage potential and flow rate ranged between 2kV to 5.5kV and 1 to 16 µl/min respectively during experimentation. The flow rate was implemented using a backpressure system which avoided the pulsing seen in most screw based syringe pumps.

The separation height between the source nozzle and the thermal exchange surface was defined using a micro-positioning xyz optical stage (Fig 2). The separation height was varied between H=2.5 mm to 17.5mm at 2.5mm increments

Five nozzle sizes were investigated; d = 0.108 mm, 0.180 mm, 0.330 mm, 0.712 mm and 1.066 mm. H and d were chosen in order to investigate electrospray cooling over a wide range of performance criteria.

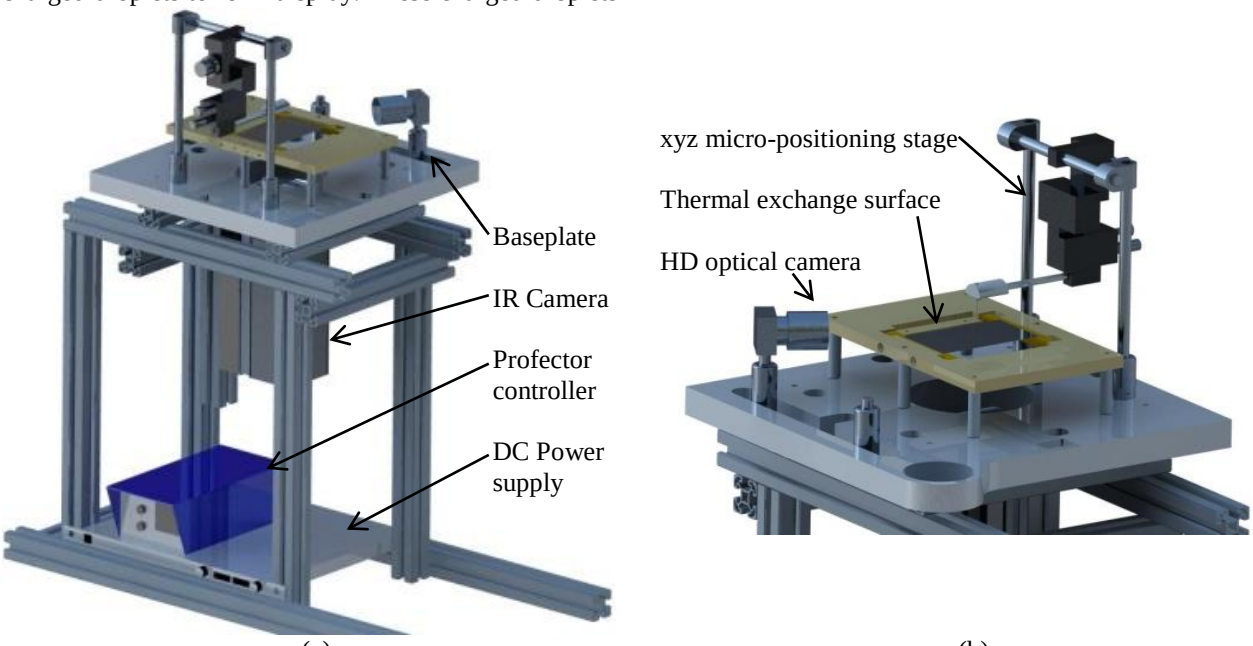

(a) (b)

Fig 2. Electrospray (a) test cell and (b) Baseplate

3.2 Heated Foil and Surrounding Structure

The baseplate (Fig 2) is constructed from 400mm x 320mm x 30mm Delrin plastic and is supported by 40mm x 40mm aluminium profile frame. The target surface (Fig 2) consists of a 115mm x 70mm x 25µm stainless steel foil bonded between two copper bus bars using electrically conductive epoxy. The copper bars are mounted to a 275mm x 180mm x 11mm polyrtheretheketone (PEEK) housing which is fixed rigidly to the Delrin baseplate.

Each bus bar has two connections on each end to which DC current was supplied from a DC power supply. The power supply has the capability of providing 8 Volts and 100 Amps in either constant voltage or constant current modes. One set of bus bars is rigidly fixed to the PEEK while the others are spring loaded to tension the foil. This tensioning system ensured that the foil remained taut for varying wall heat fluxes.

The underside of the foil was coated with a thin layer of matt black paint with an emissivity ε = 0.9 so as to minimize the effects of reflection and provide a surface of known emissivity. This facilitated accurate temperature measurement of the foil using the thermal imaging system.

3.3 Imaging System

The imaging system consisted of two parts; a high definition optical camera and a thermal imaging camera. The optical camera was used to focus on the nozzle tip and to define when the cone-jet regime of spraying had been induced.

A FLIR A-40 infrared camera using ThermaCAM Researcher PRO 2.9 software were operated in tandem to capture and record the thermal footprint of the electrospray. The total camera viewing area was 15.2 mm by 11.4 mm with a spatial resolution of 47.5 µm and a frame rate up to 50 Hz and was mounted to the aluminium profile frame directly below the thermal exchange test surface (Fig 2). For each pixel, 3 sets of 500 images at 50Hz were recorded. These sets were taken at one minute intervals and were initialized once steady state conditions were reached. All recorded results were processed using Matlab.

3.4 Working Fluid

All tests were conducted with pure ethanol, with a boiling point of 78.37^0C. Ethanol possess a low surface tension and favorable electrical conductivity. These fluid characteristics ensured the electric forces are much stronger than the intermolecular forces within the fluid. This enabled the onset of a stable cone jet regime of electrospraying at relatively low applied voltages.

Water and other fluids with greater surface tension are not suitable for the purpose of electrospraying as the voltage potential required for spraying of the liquid is close to that of the electrical coronal discharge of air under atmospheric conditions [1].

All experiments were conducted at atmospheric pressure and room temperature once steady state conditions were reached. The thermal exchange surface

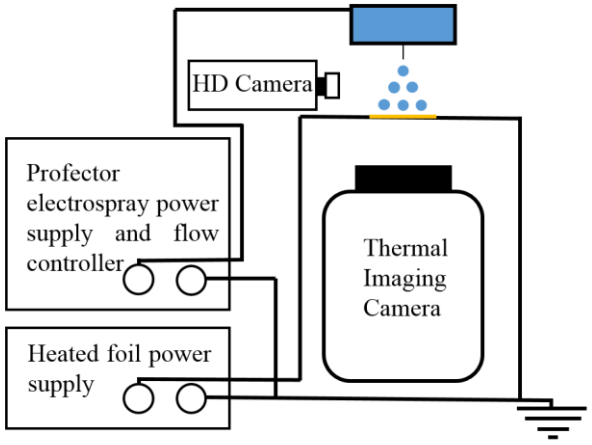

Fig 3 Experimental Rig Schematic

temperature was calculated to be uniform across its thickness and was investigated across a target surface heat flux condition of 1,082.6 W/m^2. Lateral conduction within the foil was shown to be negligible using a Finite Element model created using COMSOL Multiphysics 4.3.

4 RESULTS AND DISCUSSION

4.1 Data reduction

The local heat transfer coefficient was calculated using the expression:

$$h = q''/\Delta T \tag{1}$$

where ΔT is the temperature difference between the foil and that of the fluid. q'' is the heat flux and is assumed uniform across the thermal exchange surface since lateral conduction was deemed negligible. It is determined from the current passing through the foil, I, the resistivity of the foil, R, and the surface area, A_s, of the thermal exchange surface.

$$q'' = I^2R/A_s \tag{2}$$

In analyzing the recorded results an energy balance was implemented at each node on the thermal exchange surface and is given by:

$$q''_{EC} = q''_{Gen} - q''_{Rad\_total} - q''_{Conv} \tag{3}$$

where q''_{EC} is the heat dissipated by the electrospray cooling, q''_{Gen} is the heat generated, q''_{Rad_total} is the radiation from the top and bottom sides of the foil and q''_{Conv} is the thermal energy dissipated by natural convection from the bottom surface.

As the electrospray is axisymmetric about its nozzle centre, one can consider the concept of a radial heat transfer enhancement region. The region is measured as a distance radially outward from the projected centre of the nozzle. This area of enhancement is defined as the region where a minimum 100% increase in local wall heat transfer is observed in comparison to the no-spray,

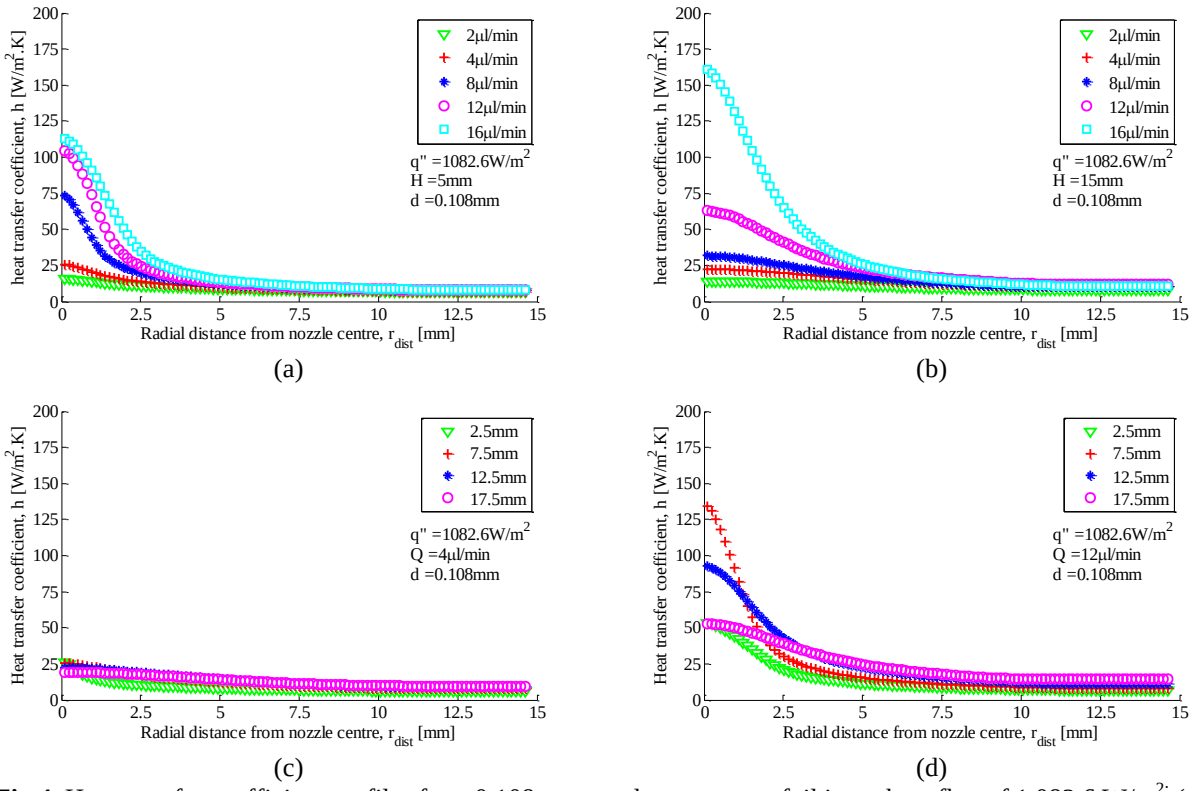

Fig 4 Heat transfer coefficient profiles for a 0.108mm nozzle at constant foil input heat flux of 1,082.6 W/m$^{2:}$ (a) – (b) depict set distances to target for increasing flow rates, Q; (c) – (d) show set flow rates with increasing H.

natural convection case. The enhanced cooling region is then calculated as:

$$r_{enh} = r_{@2q"NC} \tag{4}$$

The enhancement ratio (er) is defined as the ratio between the peak heat transfer coefficient (h_{peak}) achieved by the electrospray cooling compared to the no-spray, natural convection case (h_{NC}):

$$er = h_{peak}/h_{NC} \tag{5}$$

The electric field can be calculated by approximating it as the field between a hyperboloid and plate [5, 11]:

$$E_0 = 4V/(D_0 ln(8H/D_0)) \tag{6}$$

where V is the applied voltage to the nozzle source to induce the Taylor cone, D_0 is the outer diameter of the source nozzle, H is the separation distance of the source nozzle to the thermal exchange surface.

4.2 Electrospray radial cooling profile

Fig 4 shows that the heat transfer coefficient profiles have a similar trend for various geometric parameters, with a bell-shaped peak at the center of the impingement zone which decreases with radial distance to the value associated with natural convection in the outer periphery. Fig 4 also highlights the effect that the separation height (H) and working fluid flow rate (Q) have on the heat transfer coefficient profiles for a constant nozzle size (d) and target surface heat flux (q''). Plots (a) - (b) show the influence of volumetric flow rate for varied values of H. For a given H and d, it was observed that an increase in flow rate results in a subsequent increase in the magnitude and spread of the heat transfer coefficient. This can be seen to the greatest extent for the H = 15mm case. For H = 5mm, Q = 12µl/min and Q = 16µl/min cases it was observed that there was considerable pooling of the cooling fluid in comparison with greater separation height conditions. For higher flow rates and closer separation heights the created droplets do not have sufficient distance to establish effective plume dispersion. As a result of this pooling, similar peak heat transfer coefficients are observed for both the 12µl/min and 16µl/min tests. From this result one can conclude that there exists a *saturation point* where subsequent increase in fluid deposition will not affect the peak heat transfer coefficient, though it will alter the cooling profile. This *saturation point* depends on the separation height, flow rate and target surface temperature.

Fig 4 (c) – (d) investigates H dependency for a constant d and Q. Comparing Fig 4 (c) and (d) it is clear that the sensitivity of the heat transfer coefficient with changing source to target separation height increases markedly with increasing flow rate. It is also evident that larger separation heights yield greater spread of the enhanced heat transfer. Both Fig. 4 (c) and (d) show an interesting trend with regard to the peak heat transfer and separation distance. Initial increase in H results in an increase in the peak heat transfer, after which it decreases with further increase. This phenomenon is attributed to a *dispersal threshold*. As the separation height increases the charged droplets have greater time over which to

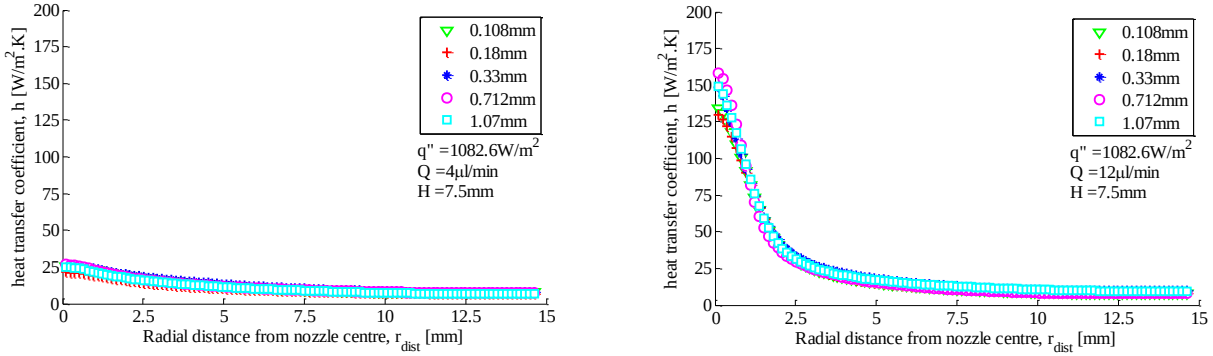

(a) (b)

Fig 7 Heat transfer coefficient profiles for a constant foil input heat flux of 1,082.6 W/m^2, a set separation height, H of 7.5mm and increasing nozzle size per series

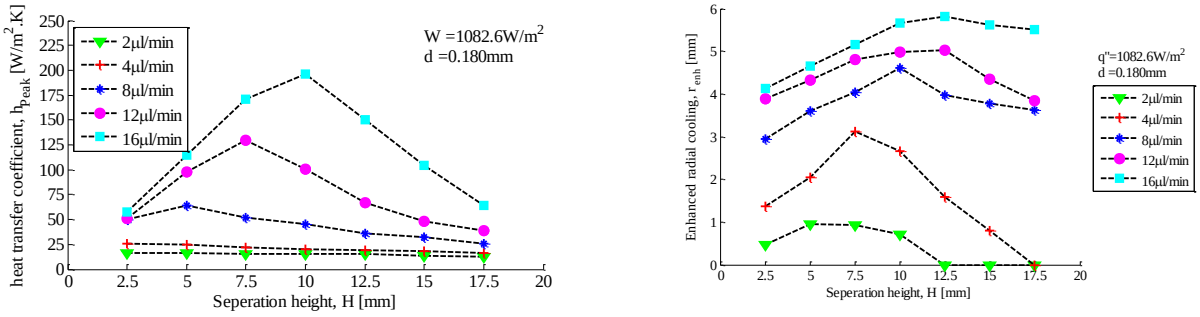

(a) (b)

Fig 8 Peak heat transfer coefficient (a) and enhance radial cooling (b) – (d) versus separation height and flow rate for a fixed wall heat flux of 1,082.6 W/m$^{2:}$

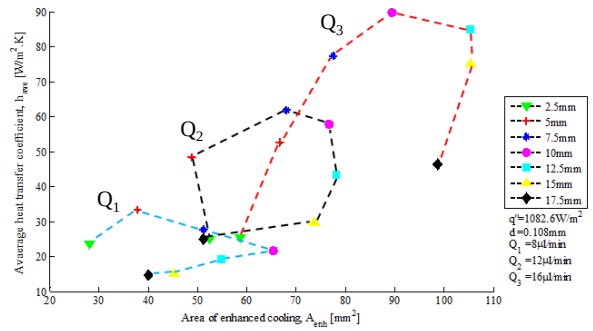

Fig 5: Average heat transfer coefficient compared with area of enhanced cooling for increasing separation heights

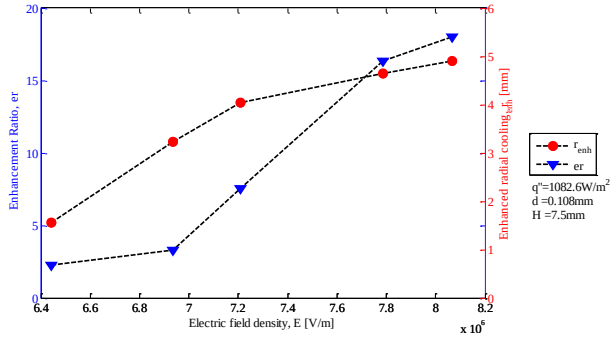

Fig 6: Enhancement ratio and region of enhanced radial cooling compared with electric field density for a fixed H, d and q$^{//}$.

repel each other which cause greater plume dispersion. This results initially in ideal two phase evaporative cooling. However as H increases further, the concentration of droplets decreases due to the increased plume dispersal. This causes less latent heat transfer resulting in a drop in the peak heat transfer. This point is further illustrated in Fig 8.

Fig 7 analyses the radial heat transfer profiles of the electrospray cooling and compares them across different values of the nozzle diameter. It is observed that both the spread and peak head transfer coefficient show little dependency on the nozzle diameter.

4.3 Peak heat transfer coefficient

Fig 8 compares the peak heat transfer coefficient, (h_{peak}) and the region of enhanced radial cooling (r_{enh}) with source to target separation height for varying flow rates and nozzle sizes. Plot 6(a)–(b) clearly demonstrates the *dispersal threshold* for the heat transfer coefficient and enhanced radial cooling respectively. For higher H and constant Q, a critical separation distance is reached after which further increase results in a decrease in both h_{peak} and r_{enh}. In Fig. 6(a) for the 2 µl/min and 4 µl/min cases the peak heat transfer coefficient is not very sensitive to H and thus the location of the maximum is difficult to judge and may in fact be lower than the minimum separation height tested, with higher flow rates demonstrating clearly the *dispersal threshold*. It is worth noting that the *dispersal threshold* point for h_{peak} and r_{enh} are not coincident at the same value of H for the same values of d, Q and q$^{//}$.

4.4 Parameter relationships

Fig 5 compares the average heat transfer coefficient (h_{ave}) with area of enhanced cooling (A_{enh}), where $A_{enh}= \pi r_{enh}^2$, for increasing values of H. The figure clearly

shows the relation between the enhanced cooling and the enhanced cooling region for varying separation heights. For the three flow rates shown the initial increase in H corresponds with an increase in both the average heat transfer and area of enhanced cooling. However a peak region of both h_{ave} and A_{enh} is reached after which they both begin to decrease. Considering the Q=12µl/min case, changing H from 2.5 mm to 7.5 mm the sharp increases are due to the electrospray cooling transitioning from saturated cooling i.e. liquid pooling, to evaporative cooling i.e. thin film evaporation. From H=7.5mm to 12.5mm the heat transfer notably decreases whilst the cooling area increases marginally. After approximately H=7.5mm the *dispersal threshold* has been passed. As discussed, this results in the mist droplets becoming very finely spread causing a drop in the h_{ave} but are still concentrated enough for the increased spreading to result in a subsequent increase in the cooling area. After H=12.5 mm both the heat transfer and the area of enhancement drop since the droplets become to finely dispersed.

Fig 6 depicts the enhancement ratio (er) and enhanced radial cooling from the source nozzle against the electric field density (E). Increasing values of E correspond to increasing values for Q (2, 4, 8, 12, 16µl/min) since it required that E be increased in order to maintain the cone-jet mode regime of spraying. The enhancement ratio shows a 's' shaped dependence on the electric field density. It is observed that as E increases er also increases. The enhancement radius, on the other hand, shows a more asymptotic relation with electric field density, due to an initial rapid increase in plume dispersion followed by gradual increases as a dispersion threshold is reached.

5 CONCLUSION

The experimental results show that the peak heat transfer coefficient, cooling profile and area of enhanced radial cooling were shown to be dependent on separation height and the cooling fluid flow rate, with little dependency on nozzle size. At lower separation heights and greater flow rates a *saturation point* was viewed where a subsequent increase in the flow rate of the working fluid yields no increase in the peak heat transfer coefficient, although the cooling profile is altered. In the case of greater separation heights and lower flow rates a *dispersal threshold* was noted where the working fluid becomes too dispersed while in transit to the target surface. The point of the dispersal threshold was shown to differ for h_{peak} and r_{enh}. The relationship between h_{ave} and A_{enh} is explored for increasing separation height and an interesting trend is observed whereby both h_{ave} and A_{enh} initially increase with increases in H after which they both begin to decrease. This illustrates the importance of the geometric configuration of the electrospray with regard to its performance as an ultra-low flow rate liquid cooling technology

ACKNOWLEDGMENTS

This work was funded in part by an EU FP7 Marie Curie grant (FP7-PEOPLE-2009-IAPP: 251349-TaylorMed). The authors also gratefully acknowledge the Irish Research Council for their support during this research project.

REFERENCES

1. Zeleny, J., *Instability of Electrified Liquid Surfaces.* Physical Review, 1917. **10**: p. 1-6.
2. Cloupeau, M. and B. Prunet-Foch, *Electrohydrodynamic spraying functioning modes: a critical review.* Journal of Aerosol Science, 1994. **25**(6): p. 1021-1036.
3. Deng, W. and A. Gomez, *The role of electric charge in microdroplets impacting on conducting surfaces.* Physics of Fluids, 2010. **22**(5): p. 1-4.
4. Inada, S. and W.-J. Yang, *Film boiling heat transfer for saturated drops impinging on a heating surface.* International journal of heat and mass transfer, 1994. **37**(16): p. 2588-2591.
5. Feng, X. and J.E. Bryan, *Application of Electrohydrodynamic Atomization to Two-Phase Impingement Heat Transfer.* Journal of Heat Transfer, 2008. **130**(7): p. 072202-072202.
6. Deng, W. and A. Gomez, *Electrospray cooling for microelectronics.* International Journal of Heat and Mass Transfer, 2011. **54**(11-12): p. 2270-2275.
7. Wang, H.C. and A.V. Mamishev, *Heat transfer correlation models for electrospray evaporative cooling chambers of different geometry types.* Applied Thermal Engineering, 2012. **40**: p. 91-101.
8. Hsiu-Che, W. and A.V. Mamishev. *Optimal heat transfer performance of the microfluidic electrospray cooling devices*. in *Semiconductor Thermal Measurement and Management Symposium (SEMI-THERM), 2011 27th Annual IEEE*. 2011.
9. Taylor, G., *Disintegration of Water Drops in an Electric Field.* Proceedings of the Royal Society of London. Series A, Mathematical and Physical Sciences, 1964. **280**(1382): p. 383-397.
10. Jaworek, A. and A. Krupa, *CLASSIFICATION OF THE MODES OF EHD SPRAYING.* Journal of Aerosol Science, 1999. **30**(7): p. 873-893.
11. Eyring, C.F., S.S. Mackeown, and R.A. Millikan, *Fields Currents from Points.* Physical Review, 1928. **31**(5): p. 900-909.